Nano Energy 65 (2019) 103988

Contents lists available at ScienceDirect

Nano Energy

journal homepage: www.elsevier.com/locate/nanoen

Full paper

Manipulation of an ionic and electronic conductive interface for highly-stable high-voltage cathodes

Sixu Deng[a,1], Biqiong Wang[a,d,1], Yifei Yuan[b,f,1], Xia Li[a], Qian Sun[a], Kieran Doyle-Davis[a], Mohammad Norouzi Banis[a], Jianneng Liang[a], Yang Zhao[a], Junjie Li[a], Ruying Li[a], Tsun-Kong Sham[d], Reza Shahbazian-Yassar[f], Hao Wang[c], Mei Cai[e,***], Jun Lu[b,**], Xueliang Sun[a,*]

[a] Department of Mechanical and Materials Engineering, University of Western Ontario, London, Ontario, N6A 5B9, Canada
[b] Chemical Sciences and Engineering Division, Argonne National Laboratory, Argonne, Illinois, 60439, USA
[c] The College of Materials Science and Engineering, Beijing University of Technology, Beijing, 100124, PR China
[d] Department of Chemistry, University of Western Ontario, London, Ontario, N6A 5B7, Canada
[e] General Motors Research and Development Center, Warren, MI, 48090-9055, USA
[f] Department of Mechanical and Industrial Engineering, University of Illinois at Chicago, Chicago, IL, 60607, USA

ARTICLE INFO

Keywords:
High voltage cathode
Hybrid Li_3PO_4–TiO_2 coating
Ionic and electronic conductivity
Side-reactions

ABSTRACT

A stable and conductive interface is one of the decisive factors in manipulating the performance of high voltage $LiNi_{0.5}Mn_{1.5}O_4$ (LNMO) cathode for Li-ion batteries. Herein, a hybrid Li_3PO_4–TiO_2 coating layer is designed as an interfacial material via controllable atomic layer deposition (ALD) on LNMO. The coating acts not just as a physical barrier to prevent the side-reactions between cathode and electrolyte at high voltage, more importantly, the hybrid coating material improves both interfacial ionic and electronic conductivities to build facile Li-ion and electron diffusion pathways for LNMO. The optimized LNMO demonstrates improved rate capability and long-life stability. The capacity retention is 81.2% comparing with 47.4% of bare LNMO at 0.5C after 300 cycles. Detailed surface structural evolution is studied via X-ray absorption near edge spectroscopy and transmission electron microscopy. This work provides new insights of hybrid interfacial design via ALD and promotes novel electrode architectures for batteries.

1. Introduction

The growing demand for high-performance Li-ion batteries has stimulated the exploration of novel electrode materials [1–3]. The development of cathode materials is crucial to Li-ion batteries moving forward, which is currently the major limiting factor of the energy density of full batteries [4–8]. Among the developed cathode materials, spinel structure $LiNi_{0.5}Mn_{1.5}O_4$ (LNMO) is one of the promising candidates due to its high operating voltage, high specific capacity, and natural elemental abundance [9]. However, it should be noted such high voltage operation also brings significant challenges to this cathode material in batteries, such as the irreversible surface phase transition, transition metal dissolution, Jahn-Teller distortion of Mn^{3+}, electrolyte oxidation, etc. [10–12] All of these challenges lead to rapid capacity decay and voltage plateau drop during cycling, resulting in unsatisfy cycling and rate performance [13,14].

Considerable efforts have been devoted to overcome these challenges, including surface coating or doping of LNMO, synthesis of novel nanostructure cathode materials, and the investigation of stable high voltage Li-ion electrolyte [9,10,15]. Among these developed strategies, coating is an effective method to avoid direct exposure of cathode materials to the electrolyte and therefore prevent the occurrence of side-reactions and the dissolution of transition metals [16–19]. On the other hand, it should be noted that for many developed coating materials, such as metal oxides, phosphates, and fluorides, to ensure the chemical and electrochemical stability at high voltage, they have limited Li^+ ionic and electron conductivity [20–22]. Therefore, introducing these inert coating materials for cathodes as a physical barrier may increase the interfacial resistance of cathodes and therefore reduce the efficiency of transformation from chemical energy to electrical energy

* Corresponding author.
** Corresponding author.
*** Corresponding author.
E-mail addresses: mei.cai@gm.com (M. Cai), junlu@anl.gov (J. Lu), xsun@eng.uwo.ca (X. Sun).
[1] These authors contribute equally to this work.

https://doi.org/10.1016/j.nanoen.2019.103988
Received 12 June 2019; Received in revised form 3 August 2019; Accepted 4 August 2019
Available online 06 August 2019
2211-2855/

of batteries in the electrochemical reaction [23–25]. As a result, despite the improvement of cycling stability of cathode LNMO, inert coating materials will sacrifice capacity, especially at high current densities.

In our previous studies, atomic layer deposited (ALD) $FePO_4$ and $AlPO_4$ were adopted as the coating layer on the modification of LNMO cathodes [26,27]. Although cycling stability were improved significantly due to the highly stability of phosphates, the sacrificial initial discharge capacity still hinders the application of these metal phosphates in high voltage LNMO cathodes because of the insufficient interfacial ionic/electronic conductivity. Employing solid-state electrolyte as coating layer by ALD, such as $LiTaO_3$, able to overcome the limited Li-ion conductivity, improving the cycling stability without loss of initial capacity [28]. However, the rate capability still has space to improve by combining with enhanced electronic conductivity [29]. Therefore, the desired interface control strategies for high voltage cathodes are urgent to be developed by designing hybrid coating materials by ALD.

In this work, we propose a novel Li_3PO_4–TiO_2 (LPO-TiO) hybrid coating material via atomic layer deposition (ALD) for LNMO. For the developed hybrid LPO-TiO coating, Li_3PO_4 is considered as a Li-ion solid-state electrolyte with promising ionic conductivity while due to the semi-conductor properties, anatase TiO_2 in the hybrid coating layer has demonstrated an enhanced electronic conductivity compared with single Li_3PO_4 [30]. Therefore, the unique hybrid LPO-TiO coating material could not only act as a physical barrier to protect the surface structure of LNMO from side-reactions, but also provide sufficient ionic and electronic conductivity for the cathode material to improve the cycling and rate performance of the batteries. Detailed physical and electrochemical characterizations of the coated LNMO are conducted. Controllable coating strategy, including optimizing coating materials and structure, with the underlying mechanism of coating effect is investigated. Synchrotron-based X-ray absorption near-edge spectroscopy (XANES) and scanning transmission electron microscopy (STEM) are employed to reveal the surface structure revolution of LNMO with the coating layer.

2. Experimental section

2.1. Preparation of LNMO electrodes

Commercial LNMO powder was purchased from Daejung Energy Materials Co., Ltd., South Korea. Electrodes were prepared by slurry casting of commercial LNMO, acetylene black (AB) and polyvinylidene fluoride (PVDF) in N-methyl-pyrrolidione (NMP) on aluminium foil and dried at 80 °C under vacuum over 12 h. The weight ratio of active materials: AB: PVDF was 80: 10: 10. The areal mass loading of active materials is 2.29–2.54 mg cm^{-2}.

2.2. Preparation of ALD LPO-TiO coated LNMO electrodes

Li_3PO_4, TiO_2, and Li_3PO_4–TiO_2 were deposited in a Savannah 100 ALD system (Ultratech/Cambridge Nanotech., USA) by using TTIP (Ti $(OCH(CH_3)_2)_4$) and water for TiO_2 cycle and LiOtBu [$(CH_3)_3COLi$] and TMPO [$(MeO)_3PO$] for LPO cycle. The deposition of the nanocomposite was carried out at 250 °C. The chosen temperature was in the overlapped temperature range of the ALD windows of TiO_2 and Li_3PO_4 to achieve ALD growth and prevented precursors from decomposing. Various ALD materials are coating on both LNMO powders and electrodes.

2.3. Characterization

The morphologies and structures of LPO-TiO coated LNMO were observed using a field emission scanning electron microscopy (FESEM, Hitachi S4800). STEM characterization was performed using an aberration-corrected JEOL JEM-ARM 200CF STEM equipped with a 200 keV cold-field emission gun, a HAADF detector and an Oxford X-max 100TLE windowless SDD X-ray detector. All synchrotron X-ray studies were carried out at the Canadian Light Source (CLS). X-ray absorption near edge structure (XANES) measurements were conducted on variable line spacing plane grating monochromator and spherical grating monochromator beamlines, respectively. The X-ray photoelectron spectroscopy (XPS) were measured with a monochromatic Al Kα source (1486.6 eV) in a Kratos AXIS Nova Spectrometer.

2.4. Electrochemical characterization

CR2032 coin cells were assembled in an argon-filled glove-box using lithium metal as the counter electrode and Celgard K2045 as the separator. The electrolyte was composed of 1 M $LiPF_6$ dissolved in ethylene carbonate (EC)-dimethyl carbonate (DMC) with a volume ratio of 1: 1. Cyclic voltammetry (CV) experiments were studied using a Biologic multichannel potentiostat 3/Z (VMP3) with a scanning rate of 0.1 mV s^{-1} and at a potential range of 3.5–5.0 V (vs Li^+/Li). Electrochemical impedance spectroscopy (EIS) tests were measured between the frequency range of 0.01 Hz–100 kHz by versatile multichannel potentiostat 3/Z (VMP3). Charge/discharge tests were carried out on the Arbin BT2000 system with a voltage range of 3.5–5.0 V. For GITT measurements, the batteries were charged with 0.2C for 15 min and rest for 1 h.

3. Results and discussion

Fig. 1a describes the proposed schematic figure of ALD LPO-TiO coating on the LNMO cathode particle. As reported in our previous study, the ALD LPO coating layer is in an amorphous state with the ionic conductivity of 1.73×10^{-7} S cm^{-1} at 323 K [31,32]. ALD crystalline anatase phase TiO_2 nano-particles are dispersed in the LPO layer [32]. The LPO solid-state electrolyte allows for facile Li-ion diffusion, while the semi-conductive TiO_2 nanoparticles form a beneficial electron pathway. STEM and synchrotron XANES are conducted to further demonstrate the proposed ALD LPO-TiO structure. To clearly show the LPO-TiO structure through TEM, 50 cycles of LPO-TiO ALD were applied resulting in a 5 nm coating, while the following electrochemical characterizations were performed using a thinner, more suitable coating thickness. As shown in Fig. 1b, the ALD LPO-TiO coating presents a clear amorphous layer with a thickness of 5 nm covered on the surface of LNMO particle. Some nanocrystalline particles of TiO_2 are dispersed in the amorphous LPO matrix layer. The lattice spacing of the plane obtained from the pixel intensity profile of the selected regions is 0.36 nm, which matches the crystal plane (101) of anatase TiO_2 [32]. It is clearly seen that the presence of Ti and P signals in EDX line-scanned spectrum (Fig. 1c), further confirming hybrid LPO-TiO coating on the surface of LNMO particle with a thickness of 5 nm. Ti L-edge and P K-edge XANES spectra are shown in Fig. 1d and e, which indicate the presence of TiO_2 and PO_4^{3-} composites in the ALD coating layer [33–35]. The feature peaks from A to D in the Ti L-edge spectrum indicate the transition of Ti 2p electrons to unoccupied 3 d electronic states. Peak A and B located at 458.2 eV and 460.2 eV, respectively, reflect the L_3-edge transition from $2p_{3/2}$ to $3d_{5/2}$ state, in which the energy gap of 2.0 eV demonstrates the characteristic of anatase structure. Features C and D, located at 463.6 eV and 465.7 eV, belong to L_2-edge transitions from $2p_{1/2}$ to $3d_{3/2}$ states [36,37]. The presence of both pre-edge and predominant peaks in P K-edge XANES spectrum correspond to phosphates [38]. Other physical characterizations, such as SEM images of bare and coated LNMO, TEM EDX elemental mapping results also demonstrate the presence of Ti and P, further confirming the successful deposition of LPO-TiO coating on LNMO particles via ALD (Supporting Figs. S1–S2). Based on the results of physical characterizations, hybrid LPO-TiO ALD coating layer is expected to improve both ionic and electronic conductivity of LNMO cathode.

Electrochemical characterizations of various coated LNMO cathodes

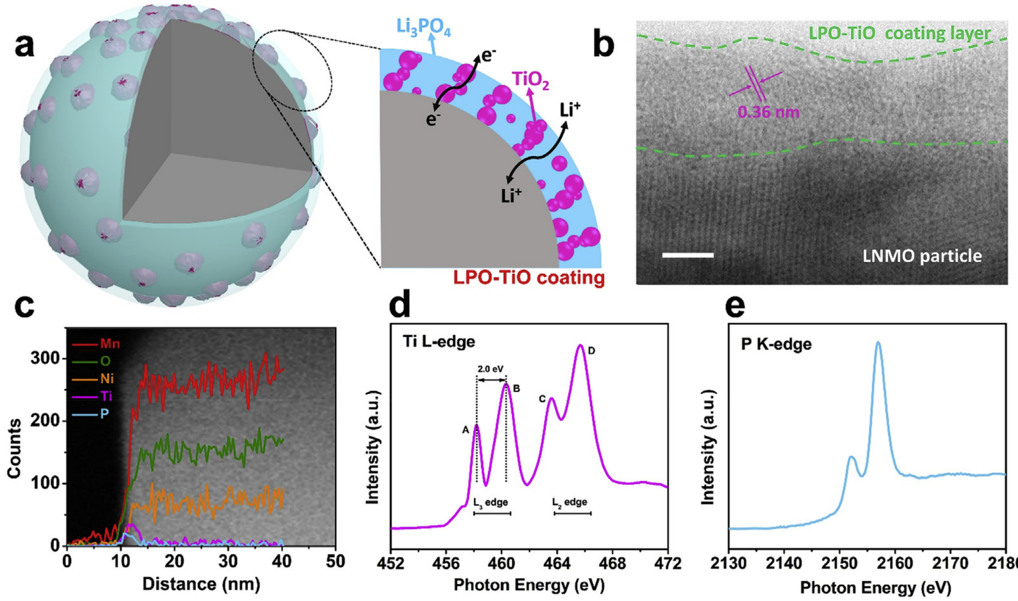

Fig. 1. Structure scheme and physical characterizations of ALD LPO-TiO coating. (a) Schematic illustration of the detailed structure of hybrid LPO-TiO coated LNMO, (b) STEM image, (c) EDX line-scanned spectrum, (d) Ti L-edge XANES and (e) P K-edge XANES of LPO-TiO coated LNMO. Scale bars, 2 nm (b).

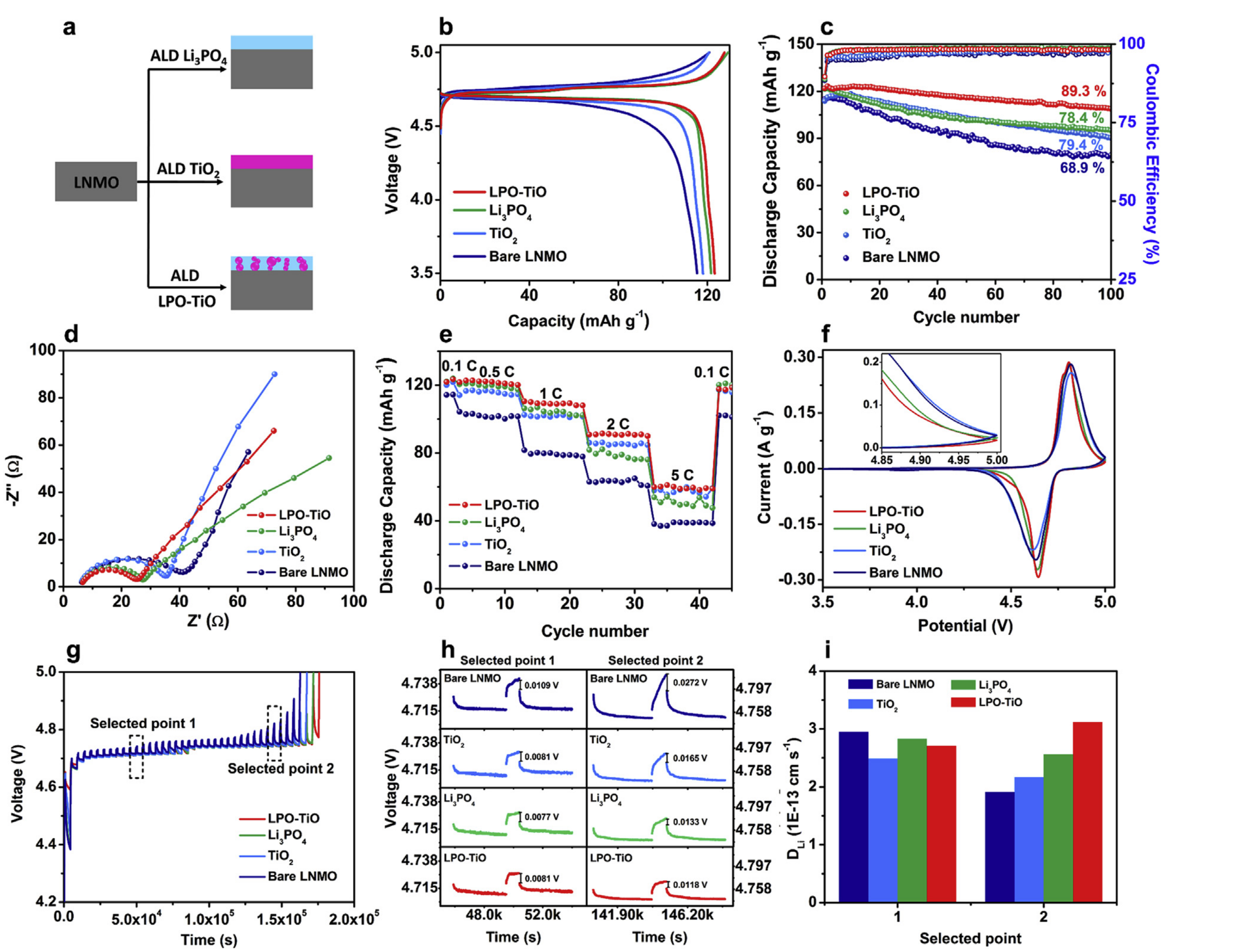

Fig. 2. Investigation the effect of various ALD coating materials on LNMO cathodes. (a) Schematic figure of various ALD coating on LNMO cathodes. (b–i) Electrochemical characterization of as-prepared LNMO cathodes: (b) Charge/discharge curves at the first cycle, (c) Cyclic performance at 0.5C, (d) EIS plots after 100 cycles, (e) Rate capability test, (f) CV curves at 0.1 mV s^{-1}, (g) Transient charge voltage profiles, (h) The corresponding polarization plots and (i) Li^+ diffusion coefficient obtained by GITT.

are illustrated in Fig. 2 and Supporting Figs. S4–S6 in order to investigate the effect of coating materials. The thickness effect of hybrid LPO-TiO coating for the performance of LNMO cathodes is firstly optimized (Fig. S4) and the 10-ALD cycle coating (around 1 nm) present the best cycling performance. Therefore, LPO-TiO coating layer of 1 nm is chosen for all of the following electrochemical characterizations. In order to investigate synergistic effect of the LPO-TiO coating for LNMO, comparisons are made between bare LNMO, hybrid LPO-TiO coated, LPO coated, and TiO_2 coated cathodes with the same coating thickness (1 nm), as shown in Fig. 2a. The first charge-discharge profiles at 0.5C are shown in Fig. 2b. Compared to bare LNMO, the LPO-TiO coated cathode shows the maximum discharge capacity with obvious reduced polarization, indicating hybrid LPO-TiO coating layer effectively improves lithium ion diffusion as well as suppressing side-reactions with the electrolyte at high voltage during charge/discharge process. Interestingly, cycling performance at 0.5C of the four cathodes shows considerable differences between the coatings (Fig. 2c). Hybrid LPO-TiO coated LNMO presents the best cycling performance where the initial discharge capacity is 121.9 mAh g^{-1} and the retention is over 89.3% (108.9 mAh g^{-1}) after 100 cycles. On the other hand, the initial capacity of bare LNMO is 115 mAh g^{-1} and the retention after 100 cycles is only 68.9%, illustrating the low cycling stability. The single LPO or TiO_2 coated LNMO cathodes demonstrate similar cycling stability that the capacity retention is about 79% after 100 cycles. In our previous study, inert ALD coating materials, such as metal oxides and metal phosphors, were widely used as the buffer layer, which improved the cycling stability of cathodes [26,27]. Nevertheless, the initial discharge capacity was lower than the bare electrode due to the reduced ionic and electronic conductivity of these ALD coatings. However, for the LPO-TiO coated LNMO, both the initial discharge capacity and cycling stability are improved comparing with bare LNMO. It indicates this unique coating does not act only as physical buffer layer. More importantly, it provides enhanced ionic and electronic conductivity for the cathode to improve the electrochemical reaction kinetics. Corresponding coulombic efficiency is also shown in Fig. 2c. The initial coulombic efficiency is around 90% for all four cathodes. After the 1st cycle, the coulombic efficiency of both LPO-TiO and LPO coated LNMO cathodes rises quickly to 98.5% within 10 cycles. However, the TiO_2 coated and bare LNMO cathodes demonstrate a lower coulombic efficiency at the first 40 cycles and then gradually increase to 96–97% in the following cycles. The differences of coulombic efficiency demonstrate the excellent ionic conductivity and electrochemical stability of the LPO coating layer for LNMO cathodes. On the other hand, TiO_2 coating layer with low ionic conductivity needs longer cycling time to stabilize and re-construct the surface structure to facile Li-ion penetration. For bare LNMO, severe side-reactions with electrolyte lead to the low coulombic efficiency and rapidly decaying cycling capacity [39,40]. EIS plots of the above four LNMO cathodes after 1, 50, and 100 cycles are shown in Figs. S7, S8, and 2d, the smallest interfacial resistance of the battery with LPO-TiO coated LNMO cathode further demonstrates the stable and conductive surface of the cathode with the support of hybrid LPO-TiO coating layer during the continued charge/discharge cycling.

Rate performance of the four cathodes is illustrated in Fig. 2e. The rate capability of cathode material is directly related to the ionic and electronic conductivity at the interface between electrode and electrolyte. Impressively, the LPO-TiO coated LNMO demonstrates significantly improved rate performance than the bare or single LPO/TiO coated cathodes. Even at 2C and 5C, the LPO-TiO coated LNMO still delivers the capacity over 90 and 60 mAh g^{-1}, which is over 60% of bare LNMO. The significant improvement of rate performance is contributed by the synergistic effect of Li_3PO_4 and TiO_2, enhancing electronic and ionic conductivity at the same time to build a smooth ion and electron diffusion way between LNMO and electrolyte. CV profiles of the four cathodes are shown in Fig. 2f. Interestingly, LPO-TiO coated LNMO demonstrates the lowest anodic peak potential (4.80 V) and highest cathodic peak potential (4.64 V) compared to other cathodes, indicating the highest electrochemical reaction activity of battery with lower resistance. Furthermore, as shown in the insert figure, LPO-TiO coated LNMO also demonstrates the lowest current at the cut-off voltage (5 V), which indicates a smaller potential polarization at a high operating voltage of the battery.

Finally, the galvanostatic intermittent titration technique (GITT) is employed to further investigate the origin of improved electrochemical properties of hybrid LPO-TiO coating layer. Transient voltage curves and the corresponding polarization and Li^+ diffusion coefficient are plotted in Fig. 2g–i. Two charging plateaus can be clear seen in the transient voltage curves of four cathodes, originating from two redox couples of Ni^{2+}/Ni^{3+} and Ni^{3+}/Ni^{4+}, respectively. Hybrid LPO-TO coated LNMO demonstrates the highest capacity and the lowest charging potential. Two selected points at the different charging plateaus are used to evaluate the polarization and capability of Li^+ diffusion of various LNMO cathodes at different charging stage. Compared to bare LNMO, the increasing of polarization potential is significantly retard in hybrid LPO-TiO coated LNMO, which indicates the side-reactions during charging process can be effectively suppressed by coating layer. Interestingly, bare LNMO exhibits the highest Li^+ diffusion coefficient at the first point, but decrease significantly during the continued charging process. However, the Li^+ diffusion coefficient in hybrid LPO-TiO increase with the deeper of charging, which is opposite comparing with bare and single LPO/TiO_2 coated LNMO. These results demonstrate hybrid LPO-TiO coating layer does not impede the Li^+ transformation within the LNMO particles. More important, it facilitates ionic migration during the charging process because of its capability to construct a stable interface to suppress side-reactions and also improve the ionic and electronic conductivity for the cathode electrode. Based on the obtained electrochemical results, LPO-TiO coating promotes higher cycling capacity and improved stability of LNMO compared to the bare or single LPO/TiO coated LNMO. LPO-TiO coating also demonstrates promising rate performance for LNMO with smaller potential polarization and battery resistance during cycling.

Controllable ALD synthetic process with various LPO/TiO growth sequences is further investigated to demonstrate the unique structural properties of the developed hybrid LPO-TiO coating for LNMO cathodes. As presented in Fig. 3a, different ALD growth sequences result in alternative coating structures. No matter what ALD sequence is employed, the fundamental design of layer-by-layer LPO + TiO (or TiO + LPO) coating is different from the synchronous growth of hybrid LPO-TiO coating layer. Although depositing with the same thickness of 1 nm, the layer-by-layer structure, which is composed by 0.5 nm LPO coating layer and 0.5 nm TiO coating layer, blocks the Li-ion or electron path-way that cannot provide continuous ionic or electronic conductivity for cathode at the same time. Especially for high-rate cycling performance, the LPO-TiO hybrid structure is proposed to have the edge over the layer-by-layer structure to build an ionic and electronic conductive interface for LNMO. Fig. 3b describes the cycling performance of LNMO cathodes with as-prepared ALD coatings at 0.5C. All of the coated cathodes demonstrate improved cycling stability compared to the bare LNMO because the ionic and electronic conductivity are not the determining factor for the discharge capacity and cycling stability at such low current density. EIS plots of the above four LNMO cathodes after 100 cycles are shown in Fig. S9, all modified LNMO cathodes demonstrate reduced interfacial resistance comparing with the bare LNMO cathode, indicating both hybrid and layer-by-layer coating layer are able to suppress the side-reactions with electrolyte. Impressively, the four cathodes demonstrate significant different rate capability as shown in Fig. 3c. The hybrid LPO-TiO coated LNMO presents the best rate performance that the capacity at 2C (91.4 mAh g^{-1}) and 5C (60 mAh g^{-1}) is much higher than the other three cathodes. The performance differences are from the distinct structural mechanisms of the ALD coatings. As aforementioned, the hybrid LPO-TiO coating enables to improve the electronic and ionic conductivity at the same time for LNMO, facilitating the electrochemical reaction transformation at high

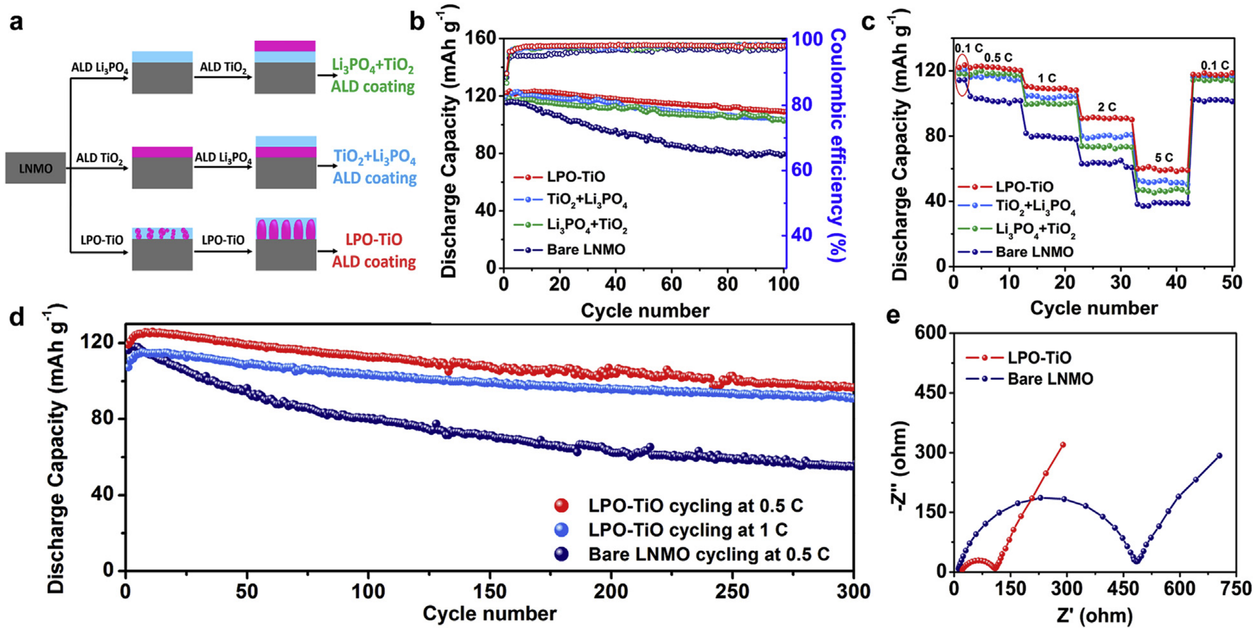

Fig. 3. Investigation of ALD coating structure effect on LNMO cathodes. (a) Schematic figure of different coating sequences of LPO and TiO during the ALD process. (b–e) Electrochemical characterization of as-prepared LNMO cathodes: (b) Cyclic performance at 0.5C, (c) Rate capability performance, (d) Long cycling stability of bare and hybrid LPO-TiO coated LNMO, and (e) EIS plots after 300 cycles of bare and hybrid LPO-TiO coated LNMO.

current density. For layer-by-layer structured LPO + TiO (or TiO + LPO) coating, there is not a continuous Li-ion or electron pathway for LNMO cathode and therefore presenting limited high-rate capacities. Long-cycling performance at different current densities of hybrid LPO-TiO coated LNMO is present in Fig. 3d. The coated cathode demonstrates a stable and prolonged cycle life at 0.5C over 300 cycles with the capacity retention of 81.2%. The capacity decay is only 0.075 mAh g^{-1} per cycle. On the contrary, the capacity retention of bare LNMO is only 47.4% after 300 cycles at 0.5C with capacity decay of 0.204 mAh g^{-1} per cycle, which is 2.72 times worse than the hybrid LPO-TiO coated LNMO. Even at 1C, the battery with coated LNMO still demonstrates very stable and high cycling capacity, where the capacity retention is 84.7% even higher than that of at 0.5C. EIS plots of the batteries after 300 cycles are investigated in Fig. 3e. Interestingly, the hybrid LPO-TiO coated LNMO present a much smaller interfacial resistance than the bare one, confirming the design concept of hybrid LPO-TiO that protect LNMO to minimize unwanted side-reactions on the surface during cycling.

In order to further unveil the phase transformation mechanism and the change of surface chemical states upon charging/discharging, Mn L-edge XANES of the LNMO cathodes is collected before and after cycling using total electron yield mode (TEY) shown in Fig. 4. The TEY mode manifests information from the surface region with a depth of around 5 nm [41,42]. Before cycling, the four as-prepared LNMO cathodes present nearly identical spectra. The spectra consist of well-separated L_2 and L_3 absorption features, resulting from the 2p core-hole spin-orbital splitting [43,44]. The predominant peaks at 645.9 eV and 648.6 eV attributing to L_3-edge and the broader peak belonging to L_2-edge in the spectra can be assigned to Mn^{4+}. The unchanged spectra of the four LNMO cathodes indicate that the Mn species existed in similar chemical environment in the close surface region before and after ALD coating. However, the spectra of cycled cathodes demonstrate significant differences, as shown in Fig. 4b. The spectrum of the bare LNMO cathode shows two new peaks at 647.2 eV and 645.4 eV that can be assigned to Mn^{3+} and Mn^{2+}, respectively, while the previous predominant Mn^{4+} peaks are nearly disappeared. The formation of Mn^{3+} derives from the Jahn-Teller distortion and oxidation of electrolyte during charge/discharge processes [44]. The following disproportionation reaction triggers the reduction of Mn from trivalence to bivalence, which takes place at the interface of cathode and electrolyte [45]. Mn^{2+} is easy to dissolve into the electrolyte, and further migrate through the separator then depositing on the surface of anode [46–48]. Meanwhile, transition metals (TMs) can facilitate the decomposition of electrolyte, which accelerate side-reactions during cycling [26,49]. All of these phase

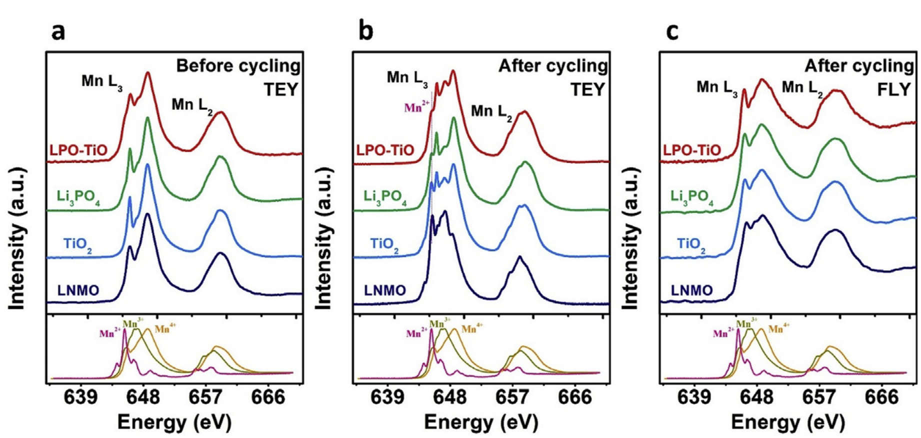

Fig. 4. Understanding the surface chemical structure evolution of LNMO cathodes before and after the electrochemical reaction. Mn L-edge XANES spectra of bare, TiO_2, Li_3PO_4, and LPO-TiO coated LNMO. (a) Before charge/discharge cycling collected at TEY mode, (b–c) After 100 charge/discharge cycles collected at TEY and FLY mode, respectively.

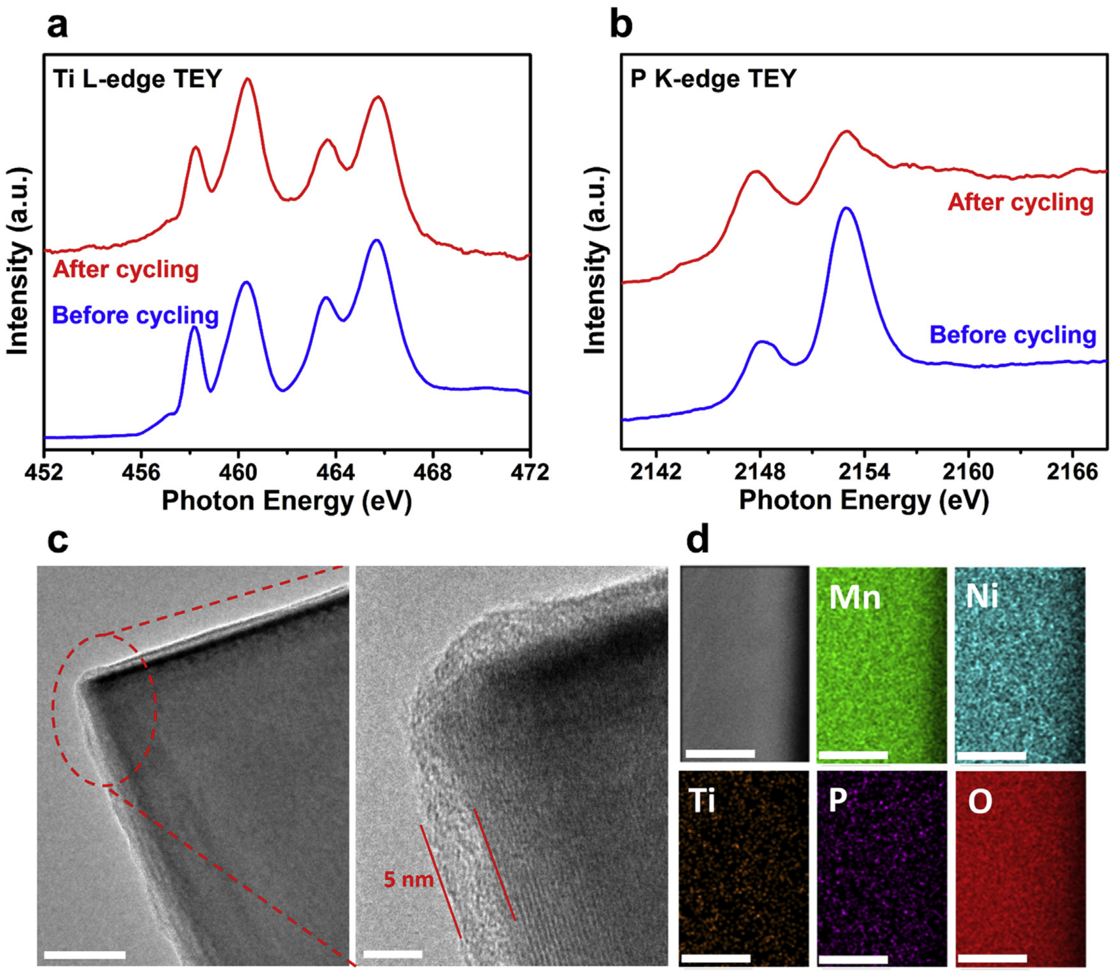

Fig. 5. Post-characterizations of hybrid LPO-TiO coated LNMO cathode after battery cycling. (a) Ti L-edge and (b) P K-edge XANES spectra of hybrid LPO-TiO coated LNMO before and after charge/discharge cycling, (c) STEM image (scale-bar 40 nm) with selected enlarged region (scale-bar 5 nm) and (d) STEM-HAADF image and the corresponding EDS mapping (scale-bar 25 nm) of hybrid LPO-TiO coated LNMO after charge/discharge cycling.

evolution results in the structural degradation of LNMO at the surface and cycling capacity decay of batteries. On the contrary, all three coated LNMO cathodes still maintain the predominant peaks of Mn^{4+} after cycling, although Mn^{3+} peaks still could be found in the spectra of the coated LNMO cathodes after cycling, which indicates that the surface side-reaction of LNMO can be suppressed to some extent but still cannot totally avoid even with the ALD coating materials. Interestingly, the intensity of Mn^{3+} peak in Li_3PO_4 coated LNMO is lower than that of TiO_2 coated LNMO, which demonstrates the electrochemical stability of PO_4^{3-} at high voltage. The intensity ratio of Mn^{2+} to Mn^{4+} is much reduced compared to the bare LNMO, when coating materials are implemented on the surface of LNMO particles. Only a shoulder peak of Mn^{3+} can be found in LPO-TiO coated LNMO cathode, indicating that the hybrid LPO-TiO coating can effectively suppress continued side-reactions with the electrolyte and help to avoid the Mn^{2+} dissolution during cycling. The XPS spectra of Li metals from both bare and LPO-TiO samples are shown in Fig. S12. The Mn peak can be detected from the surface of Li metal in bare sample, while no signal of Mn from LPO-TiO sample can be observed after cycling. This result further indicates Mn dissolution and deposition on the surface of Li metal due to lack of the protection of coating layer on the surface of cathodes. The bulk sensitive XANES spectra of LNMO cathodes collecting by fluorescence yield mode (FLY) are shown in Fig. 4c. The bulk Mn of bare LNMO after cycling also presents the weak Mn^{3+} peak in the spectrum, indicating electrolyte persistently destroying the inner structure of LNMO particles without any coating protection. On the contrary, all of the FLY spectra of coated cathodes are similar to the spectra before cycling (Fig. 4a), indicating the good protection of the LNMO bulk structure by ALD coating.

XANES and STEM characterizations are conducted to further investigate the structure and chemical state stability of hybrid LPO-TiO coating layer during cycling. Fig. 5a and b shows the Ti L-edge and P K-edge XANES in TEY mode of hybrid LPO-TiO coated LNMO cathode before and after cycling. Impressively, the spectra are nearly identical before and after battery operation, indicating the chemical stability of the coating layer during cycling. (S)TEM and corresponding EDS mapping are shown in Fig. 5c and d. It should be noted that the sample for TEM characterization is using the ALD LPO-TiO coating of 5 nm in thickness, which is the same sample employed in Fig. 1b. The ALD LPO-TiO hybrid coating layer after battery operation is still conformally coated on the surface of LNMO particle with an approximate thickness of 5 nm, which is consistent with the TEM result of ALD coating layer before cycling (Fig. 1b). EDX elemental mapping also demonstrates the presence of Ti and P elements on the surface of LNMO particle, further confirming the chemical stability of hybrid LPO-TiO coating layer in high voltage battery operation.

4. Conclusions

In conclusion, we demonstrate a controllable LPO-TiO hybrid coating material via ALD for the high voltage LNMO cathode in Li-ion batteries. The novel coating is not only as a simple physical barrier to avoid the side-reactions between cathode and electrolyte at high operating voltage. More importantly, the hybrid LPO-TiO coating layer enables enhanced ionic and electronic conductivity for the cathode that builds a stable solid-state interface between cathode and electrolyte to allow smooth Li-ions and electrons transportation. The initial capacity of the coated LNMO cathode increased from 110 mAh g^{-1} to 122 mAh g^{-1} comparing with bare LNMO, and the cycling capacity retention is over 89.3% after 100 cycles at 0.5C. Furthermore, the long cycling performance of LNMO cathode for 300 cycles at high current density also presents the significant improvement with the support of LPO-TiO coating. The capacity decay of 0.075 mAh g^{-1} per cycle with 81.2% capacity retention is obtained at 0.5C, which is only 0.37 times compared to bare LNMO. Even at 1C, hybrid LPO-TiO coated sample still demonstrates the capacity retention of 84.7%, which is 1.79 times higher than that of bare LNMO at 0.5C. The excellent electrochemical performance indicates the prolonged cycle life of LNMO cathode with the advanced coating material. TEM and synchrotron XANES characterizations further investigate the evolution of LNMO surficial phase and LPO-TiO coating structure during cycling, which demonstrate that hybrid LPO-TiO coating has sufficient chemical stability to effectively suppress the cathode surface structure degradation and dissolution of transition metals. Compared with traditional inert coating materials, it is believed that our design of the conductive LPO-TiO hybrid coating by ALD will open up new opportunities for next-generation high energy Li batteries. We hope the revelation of hybrid interfacial design via ALD and other techniques will trigger increased research interests in high-energy batteries and promote novel electrode architectures for energy storage systems.

Acknowledgements

This research was supported by the Natural Sciences and Engineering Research Council of Canada, General Motors R&D Center at Warren (GM), the Canada Research Chair Program (CRC), the Canada Foundation for Innovation (CFI), Canadian Light Source (CLS) at the University of Saskatchewan, the University of Western Ontario (UWO), and Argonne National Laboratory. Jun Lu gratefully acknowledges support from the US DOE, Office of Energy Efficiency and Renewable Energy, Vehicle Technologies Office. Argonne National Laboratory is operated for DOE Office of Science by UChicago Argonne, LLC, under contract DE-AC02-06CH11357. This work made use of the JEOL JEM-ARM200CF in the Electron Microscopy Service (Research Resources Center, University of Illinois at Chicago). R. Shahbazian-Yassar acknowledges the financial support from National Science Foundation DMR-1620901.

Appendix A. Supplementary data

Supplementary data to this article can be found online at https://doi.org/10.1016/j.nanoen.2019.103988.

References

[1] P.G. Bruce, B. Scrosati, J.M. Tarascon, Angew. Chem. 47 (2008) 2930–2946.
[2] K. Xu, Chem. Rev. 104 (2004) 4303–4418.
[3] P. Yan, J. Zheng, J. Liu, B. Wang, X. Cheng, Y. Zhang, X. Sun, C. Wang, J.-G. Zhang, Nat. Energy 3 (2018) 600–605.
[4] J. Cabana, L. Monconduit, D. Larcher, M.R. Palacin, Adv. Mater. 22 (2010) E170–E192.
[5] L. Li, X. Zhang, M. Li, R. Chen, F. Wu, K. Amine, J. Lu, Electrochem. Energy Rev. 1 (2018) 461–482.
[6] R. Schmuch, R. Wagner, G. Hörpel, T. Placke, M. Winter, Nat. Energy 3 (2018) 267–278.
[7] X. Xu, H. Huo, J. Jian, L. Wang, H. Zhu, S. Xu, X. He, G. Yin, C. Du, X. Sun, Adv. Energy Mater. (2019) 1803963.
[8] U.-H. Kim, J.-H. Kim, J.-Y. Hwang, H.-H. Ryu, C.S. Yoon, Y.-K. Sun, Mater. Today 23 (2019) 26–36.
[9] B. Xiao, X. Sun, Adv. Energy Mater. 8 (2018) 1802057.
[10] C. Zhan, T. Wu, J. Lu, K. Amine, Energy Environ. Sci. 11 (2018) 243–257.
[11] M. Hirayama, H. Ido, K. Kim, W. Cho, K. Tamura, J. Mizuki, R. Kanno, J. Am. Chem. Soc. 132 (2010) 15268–15276.
[12] C. Zhan, J. Lu, A. Jeremy Kropf, T. Wu, A.N. Jansen, Y.K. Sun, X. Qiu, K. Amine, Nat. Commun. 4 (2013) 2437.
[13] Y. Ding, Z.P. Cano, A. Yu, J. Lu, Z. Chen, Electrochem. Energy Rev. 2 (2019) 1–28.
[14] U.-H. Kim, H.-H. Ryu, J.-H. Kim, R. Mücke, P. Kaghazchi, C.S. Yoon, Y.-K. Sun, Adv. Energy Mater. 9 (2019) 1803902.
[15] D. Kim, S. Park, O.B. Chae, J.H. Ryu, Y.-U. Kim, R.-Z. Yin, S.M. Oh, J. Electrochem. Soc. 159 (2012) A193–A197.
[16] J. Chong, S. Xun, J. Zhang, X. Song, H. Xie, V. Battaglia, R. Wang, Chem. Eur J. 20 (2014) 7479–7485.
[17] S. Zhao, B. Sun, K. Yan, J. Zhang, C. Wang, G. Wang, ACS Appl. Mater. Interfaces 10 (2018) 33260–33268.
[18] S. Zhao, K. Yan, P. Munroe, B. Sun, G. Wang, Adv. Energy Mater. 9 (2019) 1803757.
[19] X.-D. Zhang, J.-L. Shi, J.-Y. Liang, Y.-X. Yin, J.-N. Zhang, X.-Q. Yu, Y.-G. Guo, Adv. Mater. 30 (2018) 1801751.
[20] H.-B. Kang, S.-T. Myung, K. Amine, S.-M. Lee, Y.-K. Sun, J. Power Sources 195 (2010) 2023–2028.
[21] J.-H. Cho, J.-H. Park, M.-H. Lee, H.-K. Song, S.-Y. Lee, Energy Environ. Sci. 5 (2012) 7124.
[22] F. Cheng, Y. Xin, Y. Huang, J. Chen, H. Zhou, X. Zhang, J. Power Sources 239 (2013) 181–188.
[23] W.-K. Shin, Y.-S. Lee, D.-W. Kim, J. Mater. Chem. A 2 (2014) 6863–6869.
[24] J.W. Kim, D.H. Kim, D.Y. Oh, H. Lee, J.H. Kim, J.H. Lee, Y.S. Jung, J. Power Sources 274 (2015) 1254–1262.
[25] Q. Wu, X. Zhang, S. Sun, N. Wan, D. Pan, Y. Bai, H. Zhu, Y.S. Hu, S. Dai, Nanoscale 7 (2015) 15609–15617.
[26] S. Deng, B. Xiao, B. Wang, X. Li, K. Kaliyappan, Y. Zhao, A. Lushington, R. Li, T.-K. Sham, H. Wang, X. Sun, Nano Energy 38 (2017) 19–27.
[27] B. Xiao, J. Liu, Q. Sun, B. Wang, M.N. Banis, D. Zhao, Z. Wang, R. Li, X. Cui, T.-K. Sham, X. Sun, Adv. Sci. 2 (2015) 1500022.
[28] X. Li, J. Liu, M.N. Banis, A. Lushington, R. Li, M. Cai, X. Sun, Energy Environ. Sci. 7 (2014) 768–778.
[29] F.-D. Yu, L.-F. Que, C.-Y. Xu, M.-J. Wang, G. Sun, J.-G. Duh, Z.-B. Wang, Nano Energy 59 (2019) 527–536.
[30] H. Liu, C. Chen, C. Du, X. He, G. Yin, B. Song, P. Zuo, X. Cheng, Y. Ma, Y. Gao, J. Mater. Chem. A 3 (2015) 2634–2641.
[31] B. Wang, J. Liu, Q. Sun, R. Li, T.K. Sham, X. Sun, Nanotech 25 (2014) 504007.
[32] B. Wang, J. Liu, Q. Sun, B. Xiao, R. Li, T.-K. Sham, X. Sun, Adv. Mater. Interfaces 3 (2016) 1600369.
[33] D. Vantelon, A. Hofmann, K. Hanselmann, A. M. Flank 882 (2007) 232-234.
[34] J. Prietzel, A. Dümig, Y. Wu, J. Zhou, W. Klysubun, Geochem. Cosmochim. Acta 108 (2013) 154–171.
[35] B. Kim, M. Gautier, C. Rivard, C. Sanglar, P. Michel, R. Gourdon, Environ. Sci. Technol. 49 (2015) 4903–4910.
[36] A.A. Mosquera, J.L. Endrino, J.M. Albella, J. Anal. Atomic Spectrom. 29 (2014) 736–742.
[37] A. Sharma, M. Varshney, J. Park, T.-K. Ha, K.-H. Chae, H.-J. Shin, RSC Adv. 5 (2015) 21762–21771.
[38] B. Kim, M. Gautier, C. Rivard, C. Sanglar, P. Michel, R. Gourdon, Environ. Sci. Technol. 49 (2015) 4903–4910.
[39] J.M. Tarascon, J. Electrochem. Soc. 138 (1991) 2859.
[40] K.Y. Chung, W.-S. Yoon, K.-B. Kim, X.-Q. Yang, S.M. Oh, J. Electrochem. Soc. 151 (2004) A484–A492.
[41] T. Okumura, T. Fukutsuka, K. Matsumoto, Y. Orikasa, H. Arai, Z. Ogumi, Y. Uchimoto, Dalton T 40 (2011) 9752–9764.
[42] T. Okumura, M. Shikano, H. Kobayashi, J. Power Sources 244 (2013) 544–547.
[43] F.M.F. de Groot, J.C. Fuggle, B.T. Thole, G.A. Sawatzky, Phys. Rev. B 42 (1990) 5459–5468.
[44] N.P.W. Pieczonka, Z. Liu, P. Lu, K.L. Olson, J. Moote, B.R. Powell, J.-H. Kim, J. Phys. Chem. C 117 (2013) 15947–15957.
[45] C. Zhan, J. Lu, A. Jeremy Kropf, T. Wu, A.N. Jansen, Y.-K. Sun, X. Qiu, K. Amine, Nat. Commun. 4 (2013) 2437.
[46] K.Y. Chung, W.-S. Yoon, H.S. Lee, X.-Q. Yang, J. McBreen, B.H. Deng, X.Q. Wang, M. Yoshio, R. Wang, J. Gui, M. Okada, J. Power Sources 146 (2005) 226–231.
[47] J.-H. Kim, N.P.W. Pieczonka, Z. Li, Y. Wu, S. Harris, B.R. Powell, Electrochim. Acta 90 (2013) 556–562.
[48] P.V. Sushko, K.M. Rosso, J.-G. Zhang, J. Liu, M.L. Sushko, Adv. Funct. Mater. 23 (2013) 5530–5535.
[49] W. Liu, Q. Shi, Q. Qu, T. Gao, G. Zhu, J. Shao, H. Zheng, J. Mater. Chem. A 5 (2017) 145–154.

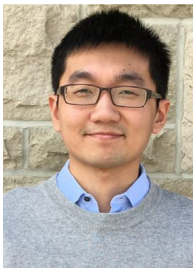

Dr. Sixu Deng is currently a Ph.D. candidate in Prof. Xueliang (Andy) Sun's Group at the University of Western Ontario, Canada. He received his B.Eng. and Ph.D. degree of Materials Science and Engineering from Beijing University of Technology in 2011 and 2018, respectively. His research interests focus on cathode materials for lithium-ion batteries, sulfide and halide solid-state electrolytes, and all-solid-state lithium-ion batteries.

Dr. Biqiong Wang is currently a researcher in the Global Research and Development Department of General Motors. She received Bachelor degree in Materials Science in 2012 at City University of Hong Kong and her Ph.D. degree in Materials Engineering from Western University, Canada. Her research interests are associated with the application of thin film deposition in batteries. Another part of her work is related to the study of energy materials via synchrotron radiation.

Dr. Yifei Yuan is currently a researcher working jointly at University of Illinois, Chicago and Argonne National Laboratory. He received his Ph.D. in Materials Science and Engineering from Michigan Technological University. His research interest is the development of advanced electrode materials for rechargeable batteries and the understanding of energy storage mechanisms using various in situ tools.

Dr. Xia Li is currently a Mitacs Postdoc Fellow in Prof. Xueliang (Andy) Sun's Group at the University of Western Ontario, Canada. She received her B.S. degree from Dalian University of Technology, China, in 2009 and M.S. degree from Nankai University, China, in 2012. She received her Ph.D. degree at the University of Western Ontario, Canada, in 2017. Her current research interests focus on lithium-sulfur batteries, Li-ion batteries, all solid-state batteries, and synchrotron based techniques.

Dr. Qian Sun is currently a Mitacs Postdoc Fellow in Prof. Xueliang (Andy) Sun's Group at the University of Western Ontario (Western Univerisity), Canada. He received his B.S. degree in Chemistry in 2006, M.S. degree in Physical Chemistry in 2009, and Ph.D. degree in Applied Chemistry in 2013 under the supervision of Prof. Dr. Zheng-Wen Fu on the study of Li-/Na-ion batteries and Na-air batteries, all at Fudan University, China. He joined Prof. Sun's group in 2013 and his current research interests focus on Na-air, Na-ion, and room temperature Na–S batteries as well as solid-state Li/Na batteries.

Kieran Doyle-Davis received his Honours BSc in Physics from McMaster University in 2018, with research focus on process optimization for lithium ion battery fabrication, and thin polymer films. Kieran is currently an MESc candidate at the University of Western Ontario under the supervision of Prof. Xueliang Sun. His current research interests include the development of next generation surface modified 3-D current collectors for both solution and solid-state lithium ion batteries.

Dr. Mohammad Norouzi Banis is a research engineer in Prof. Xueliang (Andy) Sun's group at the University of Western Ontario, Canada. He received his Ph.D. degree in 2013 in Materials Science and Engineering from Western University, on the study of nanostructured low temperature fuel cells and application of x-ray absorption spectroscopy in energy related systems. His current research interests include study of metal ion, metal air and nanocatalysts via in-situ synchrotron-based techniques.

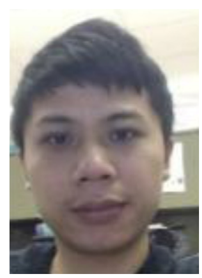

Jianneng Liang is currently a Ph.D. candidate in the department of Mechanical and Materials Engineering at the University of Western Ontario, Canada. He got his B.S. in metallurgical engineering in 2015 from Central South University, China. Currently, his research interests include solid-state polymer electrolytes, hybrid electrolyte, all solid-state LIBs and Li–S batteries, and the interfacial study in all-solid-state batteries.

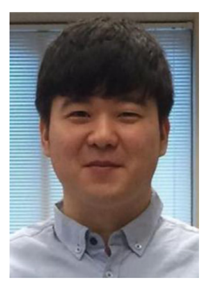

Dr. Yang Zhao is currently is a postdoctoral associate in Prof. Xueliang (Andy) Sun's Group at the University of Western Ontario, Canada. He received his B.S. degree and M.S. degree from Northwestern Polytechnical University (Xi'an, China) in 2011 and 2014, respectively. He obtained his Ph.D. degree in Materials Science and Engineering from University of Western Ontario in 2018. His current research interests focus on atomic layer deposition and molecular layer deposition for energy storage and conversion.

Junjie Li is currently a Ph.D. candidate in Prof. Xueliang (Andy) Sun's Group at the University of Western Ontario, Canada. He received his M.S. degree in physical chemistry from University of Science and Technology of China in 2017. Currently, he is working on the synthesis of advanced nanomaterials for fuel cell applications.

Ruying Li is a research engineer in Prof. Andy Xueliang Sun's group at the University of Western Ontario, Canada. She received her master degree in materials chemistry in 1999 from the University of Manchester, UK. Then she worked as a research assistant at the University of British Columbia, Canada and L'Institut National de la Recherche Scientifique (INRS), Canada. Her current research interests are focused on advanced materials and characterization for electrochemical energy storage and conversion, including electrocatalysis in fuel cells and electrodes in lithium batteries.

Prof. T.K. Sham is a Distinguished University Professor and a Canada Research Chair in Materials and Synchrotron Radiation at the University of Western Ontario. He obtained his PhD from the University of Western Ontario (1975) with a BSc from the Chinese University of Hong Kong. He joined the Chemistry Department at Brookhaven National Laboratory in 1977 and returned to Western in 1988. He is presently the Director of the Soochow-Western Centre for Synchrotron Radiation, a Fellow of the Royal Society of Canada and an Officer of the Order of Canada. Dr. Sham's expertise are nanomaterial synthesis, surface and interface, X-ray absorption related spectroscopy and microscopy. His recently focus is nanostructure phase transition, assembly of nanocomposites, in situ/in operando studies of energy materials and devices. X-ray excited optical luminescence in the energy and time domain, nanomaterials for drug delivery, and micro-beam analysis of cultural and heritage materials.

Prof. Reza Shahbazian-Yassar is an associate professor of Mechanical Engineering at the University of Illinois at Chicago. Prior to this position, he was an assistant and then associate professor at Michigan Technological University from 2007 to 2015. He received his Ph.D. in Materials Science from Washington State University in Pullman, WA, in Dec 2005. He has published more than 126 journal papers and four book chapters. His research is mainly focused on (1) in-situ TEM of functional nanomaterials; (2) material design and discovery for safe and high energy density batteries; and (3) advanced manufacturing for batteries.

Prof. Hao Wang is the professor in College of Materials Science and Engineering, Beijing University of Technology, China. Dr. Wang received his Ph.D. in applied chemistry in 1997 from Beijing Institute of Technology, China. Then he worked as a postdoctoral fellow in the Tokyo Institute of Technology, Japan. His current research interests are focused on advanced materials for electrochemical energy storage, and electrochromic materials and devices.

Dr. Mei Cai is a General Motors technical fellow and the manager of Energy Storage Materials Group at General Motors Global Research and Development Center. Dr. Cai received her Ph.D. in Chemical Engineering in 1999 from Wayne State University, Detroit, Michigan and has been with GM for 20 years. She has extensive experience in many of the advanced energy materials research area, including fuel cells, gaseous fuel storage, batteries, and capacitors. Her current research interests are focused on synthesis and processing of nanostructured materials, nanocomposite materials, and their applications in automotive clean energy areas.

Dr. Jun Lu is a chemist at Argonne National Laboratory in United States. Dr. Lu completed his Ph.D. from the Department of Metallurgical Engineering at University of Utah in 2009 with a major research on metal hybrid for reversible hydrogen storage application. His research interests focus on the electrochemical energy storage and conversion technology, with main focus on beyond Li-ion battery technology.

Prof. Xueliang (Andy) Sun is a Canada Research Chair in Development of Nanomaterials for Clean Energy, Fellow of the Royal Society of Canada and Canadian Academy of Engineering and Full Professor at the University of Western Ontario, Canada. Dr. Sun received his Ph.D. in materials chemistry in 1999 from the University of Manchester, UK, which he followed up by working as a postdoctoral fellow at the University of British Columbia, Canada and as a Research Associate at L′ Institut National de la Recherche Scientifique (INRS), Canada. His current research interests are focused on advanced materials for electrochemical energy storage and conversion.